ANALYSIS OF THE BIOMECHANICAL RESPONSE OF KIDNEYS UNDER BLUNT IMPACT

K.-U. Schmitt[1,2] and J. G. Snedeker[1]
[1]Institute for Biomedical Engineering, Swiss Federal Institute of Technology (ETH) and University of Zurich, Switzerland
[2]Working Group on Accident Mechanics (AGU), Zurich, Switzerland

ABSTRACT

This study addresses the biomechanical response of kidneys to traumatic insult by pendulum impact. Force-deformation characteristics were derived for 65 impacted adult pig kidneys. Renal injuries were classified by autopsy, and an injury risk analysis was performed. An energy based injury threshold was identified, with a strain energy density of 21 kJ/m^3 corresponding to a 50% risk of renal injury level AIS3 or higher. Finally, the impact tests were simulated using a finite element model of the human kidney to investigate underlying injury mechanisms. The model predicted the renal capsule and underlying parenchyma to first fail at an impact energy level of 4.0J, consistent with experimental results.

Keywords: Kidney, blunt impact, abdomen, biomechanics

KIDNEY INJURY is reported in 8-10% of abdominal trauma cases and is mostly sustained in automotive traffic accidents (41%) followed by sports injury and accidents at work (both 13%) [Bschleipfer et al. 2002]. Trauma must be severe to produce major renal injuries, as the kidney is well protected by its position lying high in the retroperitoneum with the abdominal viscera positioned anterior and the back muscles posterior. Therefore, only about 15-20% of renal injuries include deep parenchymal laceration and injuries to the collecting system [Schmidlin et al. 1996]. The predominant cause of such renal trauma is blunt impact [Schmitt et al. 2004].

Numerical models of blunt trauma are often employed to analyze the mechanisms underlying these injuries. Unfortunately, the dynamic mechanical properties of very soft tissues have not yet been thoroughly investigated [Miller 2000]. Some information on the properties of the renal parenchyma is available [Yamada 1970, Melvin et al. 1973, Farshad et al. 1999, Tamura et al. 2002, Snedeker et al. 2005a] as well as for the renal capsule [Snedeker et al. 2005b]. These experimental data have been fit with various numerical models suitable for implementation into numerical models of renal trauma. For example, Miller (2000) developed a three-dimensional, non-linear, viscoelastic constitutive model of the kidney that accounts for the tissue deformation behavior under compression at high strain rates that are typical for impact loading. Similar models have been developed and implemented in simulation studies of the kidney [Snedeker et al. 2002, 2005a], as well as the brain [e.g. Mendis et al. 1995], and the liver [Miller 2000, Lee and Yang 2001].

Identifying mechanisms of injury and the associated injury tolerance levels is an essential step in injury prevention, and is of critical concern when applying numerical trauma models. Several empirical injury criteria have been suggested for blunt abdominal impact, including force criteria [Stalnaker et al. 1973], compression criteria [Miller 1989], and viscous criteria [Lau and Viano 1981, Rouhana et al. 1985]. The application of failure criteria for individual abdominal organs is less common. Deformation energy, which is an accurate predictor of failure in many engineering analyses, was hypothesized to be an appropriate predictor of injury in kidneys subjected to blunt traumatic loads.

Strain energy density has been investigated as a renal injury criterion in recent study by Snedeker et al. (2005a). Here it was shown that the renal parenchyma tissues consistently fail at strain-energy density levels of 40-60 kJ/m^3, a threshold that appeared to be independent of deformation rate. The relationship between whole organ impact energy and localized tissue failure was established through finite element

analysis. The authors suggested an average, whole organ strain-energy density level of 25 kJ/m^3 as an organ level injury criterion. It should be noted that these results were obtained using falling weight impacts, as well as an unconventional projectile impact system, and that precise determination of the energy transferred to the kidney was not ensured. The present study expands on this work with an improved experimental methodology and expanded experimental scope.

The overarching goal of this study was to investigate the biomechanical response of kidneys in controlled, blunt impact, with well defined boundary conditions. As part of the biomechanical characterization, failure criteria were investigated with respect to the prediction of organ failure. To this end, adult porcine kidneys were subjected to blunt impacts using a free swinging pendulum impactor. Fully perfused organs were mounted to the test set-up and subjected to a single impact with varying impact velocity (i.e. height of the pendulum) and impact mass. Sixty-five tests were carried out, the force-deformation characteristics were analyzed, and the resulting injuries were catalogued. Observed renal injuries were classified according to the AAST renal injury scale [Moore et al. 1995]. An injury risk analysis was then performed and an energy based injury threshold was identified. In a final step, a detailed finite element model of the human renal system was implemented in an attempt to analyze the underlying mechanisms of renal injury in the experimental load case.

MATERIALS AND METHODS

All experiments were performed according to Swiss regulations for research ethics. A total of 65 porcine kidneys were obtained from the local slaughterhouse. Only kidneys with an intact capsular membrane, ureter and renal vasculature were used. All kidneys were tested within 2 to 5 hours postmortem. All impacts were performed as blunt impact to the dorsal side of the kidney, with each organ being loaded only once. The pre-impact mass of the porcine kidneys tested (after preparation, not yet perfused) was 0.175 kg ± 0.026 kg; by choosing kidneys of similar size, the comparability of results was facilitated.

The filling of the renal pelvis by organ perfusion is regarded to be important for the distribution of the forces within the kidney, with the renal pelvis acting as an incompressible support at the centre of the organ [Schmidlin et al. 1996]. Furthermore, the perfusion of the kidney fills its vascular system and thus accounts for the physiological ventro-dorsally biconvex shape that maintains capsular tension. In an attempt to recreate the natural state of organ perfusion, an infusion line was connected to the primary renal artery to perfuse the organ during testing; the solution was effused through the ureter. The vasculature of each kidney was perfused throughout the experiment with physiological buffered saline solution at a pressure of approximately 80 mmHg.

To provide a nearly frictionless contact between the kidney and rigid surfaces, the kidneys were hung within a lubricated plastic bag. The ventral surface of the kidney was flat against a rigid steel plate, and the dorsal surface was loaded horizontally by a freely swinging pendulum device at the bottom of its swing arc. The pendulum was instrumented with a single axis piezo-resistive accelerometer (Model 7270A, Endevco Inc., San Juan Capistrano, CA USA) to record the acceleration along the impact axis. Different steel right cylindrical impactors (diameter 60 mm) were used in the experiments: one weighing 4.7 kg and one weighing 2.2 kg. Figure 1 illustrates the experimental set-up.

Each impact was filmed in the sagittal plane at 1,000 Hz by a high-speed video camera (AOS Technologies AG, Baden - Daettwil, Switzerland). Both the accelerometer and the camera were triggered simultaneously, thus synchronizing the recorded accelerometer data with the captured video. The corresponding time-dependent impact force was calculated directly from the acceleration data. Organ deformation was obtained by double integration of the acceleration data and was additionally verified against video sequences that were analyzed using a tracking algorithm provided by the camera manufacturer. Pendulum impact velocity was adjusted by changing the drop height of the pendulum. The velocity of the pendulum at the moment of impact was also confirmed against evaluation of the videos.

After each impact, a thorough autopsy of each kidney was performed according to a standardized forensic protocol. Both the quantity and location of parenchymal lesions, if any, were catalogued. The

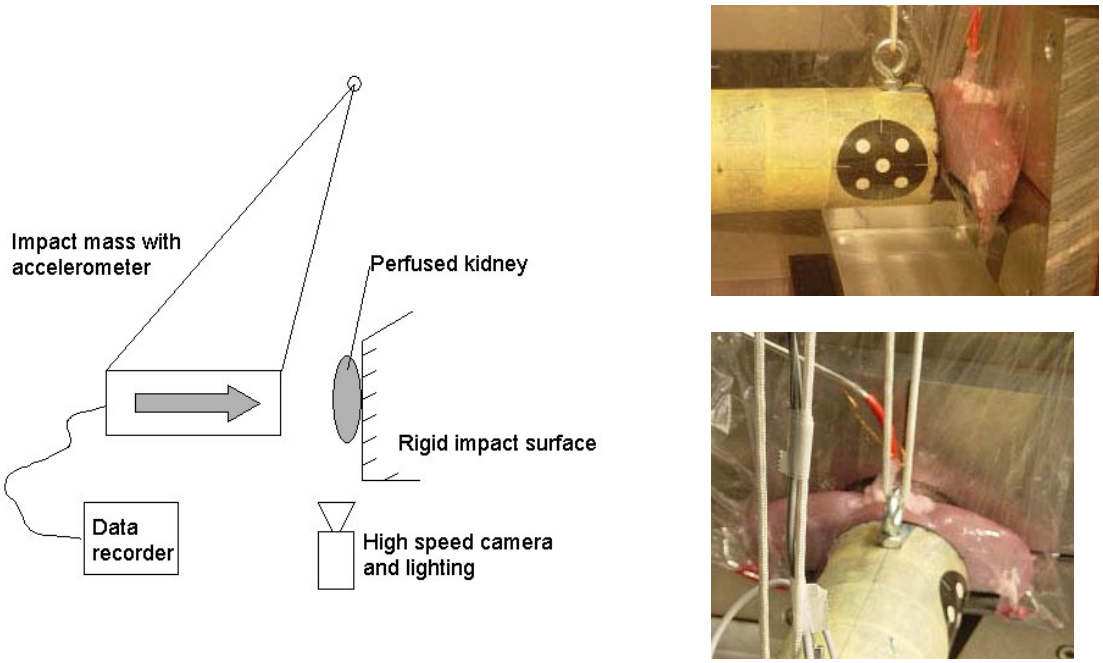

Figure 1: Schematic of the experimental set-up (left). Pictures showing the impactor and a perfused kidney (right).

renal injury scale of the American Association for the Surgery in Trauma (Table 1) was used to classify the observed injuries.

In an attempt to identify the underlying injury mechanisms for the applied load case, the pendulum impact experiments were simulated using an anatomically detailed finite element model of the isolated human renal system. The anatomy of the model was originally derived from the National Library of Medicine Visible Woman project, and then non-uniformly scaled using anatomical reference points to accord with the porcine kidneys used in the present study (130 mm long, 65 mm wide, 32 mm deep). For a detailed description of the geometric construction methods used in the development of this model, the reader is referred to Snedeker et al. (2002).

Table 1: Kidney injury scale of the American Association for the Surgery in Trauma (AAST) [Moore et al. 1995] as well as the corresponding scale on the AIS (Abbreviated Injury Scale) [AAAM 1990/1998].

AAST grade	Description of injury	Corresponding AIS grade
I	Renal contusion; Microscopic or gross hematuria, urologic studies normal; subcapsular, nonexpanding without parenchymal laceration	2
II	Nonexpanding perirenal hematoma confined to renal retroperitoneum; laceration of <1.0 cm parenchymal depth of renal cortex without urinary extravasation	2
III	Laceration of >1.0 cm parenchymal depth of renal cortex without collecting system rupture or urinary extravasation	3
IV	Parenchymal laceration extending through renal cortex, medulla, and collecting system. Injury of the main renal artery or vein injury with contained hemorrhage	4
V	Completely shattered kidney Avulsion of renal hilum which devascularizes kidney; traumatic renal arterial disruption, traumatic renal arterial occlusion	4/5

In this model, the kidney body was treated as a homogeneous structure with no anatomical distinction made between the renal cortex and the renal medulla. Since these constituent tissues have similar gross mechanical behavior [Yamada 1970, Farshad et al. 1999], treating the tissues as a single structure is a reasonable simplification of the system. The solid-fluid interactions within the kidney were simplified by treating fluids (i.e. blood and urine) as very low-shear modulus solids. The issue of parenchymal perfusion was addressed by employing a hyperelastic/ viscoelastic constitutive law that appropriately represented the mechanical behavior of soft tissues as measured in experiments on whole, perfused organs. The mechanical experiments upon which the parenchymal properties are based come from tests on anesthetized Rhesus monkeys [Melvin et al. 1973], in which the abdominal organs of the living primates were surgically mobilized and tested in uniaxial compression at deformation rates up to 5 m/s (~ 250 s^{-1}). The renal parenchyma was modeled as a second order hyperelastic material with viscoelastic behavior implemented via a single order Prony series [Snedeker et al. 2002].

The kidney parenchyma is surrounded by a thin, tough, fibrous capsule that was modeled using membrane elements sharing nodes with the underlying parenchymal elements on the surface of the kidney. A nonlinear, large-strain, rate-dependent material law was implemented with properties based upon published high speed mechanical experiments [Snedeker et al. 2005b]. The calyces and renal pelvis were modeled as a fluid-filled structure with walls consisting of an isotropic, linearly elastic, and nearly incompressible material. The material properties employed were based upon quasi-static experimental tensile tests performed on cadaveric human tissues [Yamada, 1970]. The calyces and renal pelvis were assigned a thickness of 1.0 mm, an elastic modulus of 995 kPa, and a Poisson's ration of 0.45. All blood vessels were modeled as a thin walled membrane surrounding a "fluid" represented by a very low shear modulus solid element. This solid used to represent blood and urine was assigned a bulk modulus of 420 kPa, and a shear modulus of 20 Pa. A hydrostatic arterial pressure of 100 mmHg was applied to the internal lumina of the arteries. No vessel pressure was applied to the veins. A complete description of the material laws applied to the model can be found in Snedeker et al. (2005a).

The kidney model was oriented in a configuration replicating the experimental setup used in the pendulum impact tests. The renal body was placed flat against a rigid plate support with a low coefficient of friction ($\mu = 0.05$) between the kidney capsule and the support. The impactor was modeled as a rigid body. The system was impacted at a velocities corresponding to energy levels of 1.0J, 2.0J, 3.0J and 4.0J. The resulting internal stresses, strains, and strain energy densities were then compared to experimentally observed injury patterns in an attempt to correlate these quantities to injury.

RESULTS

The force versus deformation characteristics were derived from impactor acceleration recorded within each kidney test. Typical force displacement curves are shown in Figure 2.

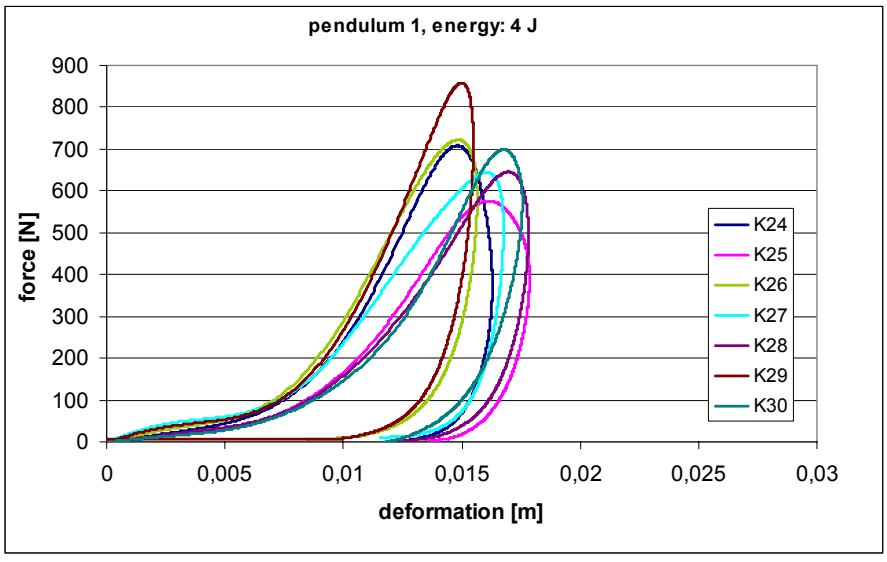

Figure 2: Results for pendulum mass 4.71 kg; impact velocity 1.3 m/s, corresponding impact energy: 4 J. The visco-elastic behavior is clearly visible. All other results are presented in the Appendix.

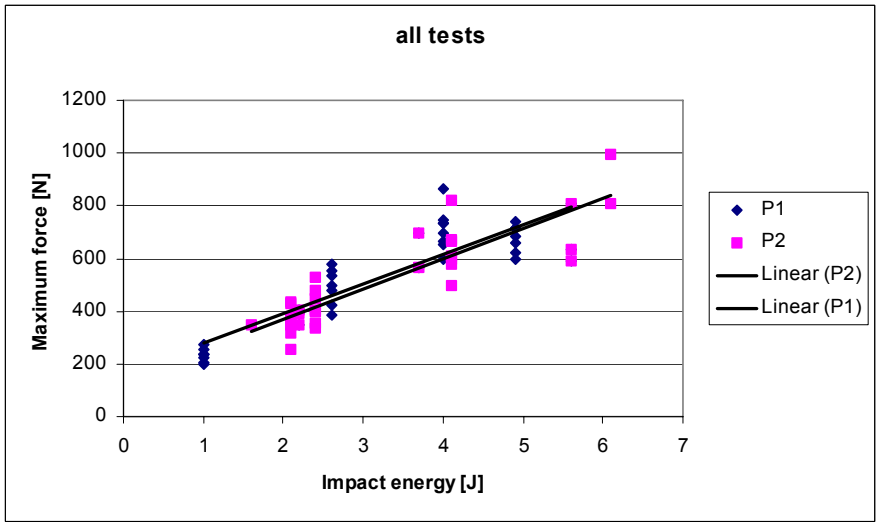

Figure 3: Maximum forces recorded with pendulum 1 (mass: 4.7 kg) and pendulum 2 (mass: 2.2.kg) at different impact energies. Trendlines indicate that the results do not depend on the pendulum mass.

The visco-elastic nature of kidney tissue is clearly demonstrated; after peak impact force, the organ unloads along a lower energy force-deformation path. It was observed that both the maximum impact force and maximum organ deformation increase with increasing impact energy. However, for impacts at 4.9 J, the maximum recorded force was slightly smaller than that at 4. 0 J. The maximum recorded forces are presented in Figures 3 and 4. The addition of linear trendlines indicated that peak impact force was dependent on impact energy without respect to the applied pendulum mass (Figure 3).

Post-impact grading of kidney injury showed an overall increase in injury severity with increasing impact energy (Figure 5). At higher impact energies the number of lacerations in the renal cortex increased and generally became deeper. Injury on the ventral side of the organ was more frequent than on the dorsal side (i.e. the impact side). Figure 6 illustrates an injury pattern typical of those observed. It was apparent that similar energy levels accounted for similar injury grading, independent of the applied pendulum mass. Thus in general, similar energy levels result in similar biomechanical response, regardless of the choice of impact mass or velocity.

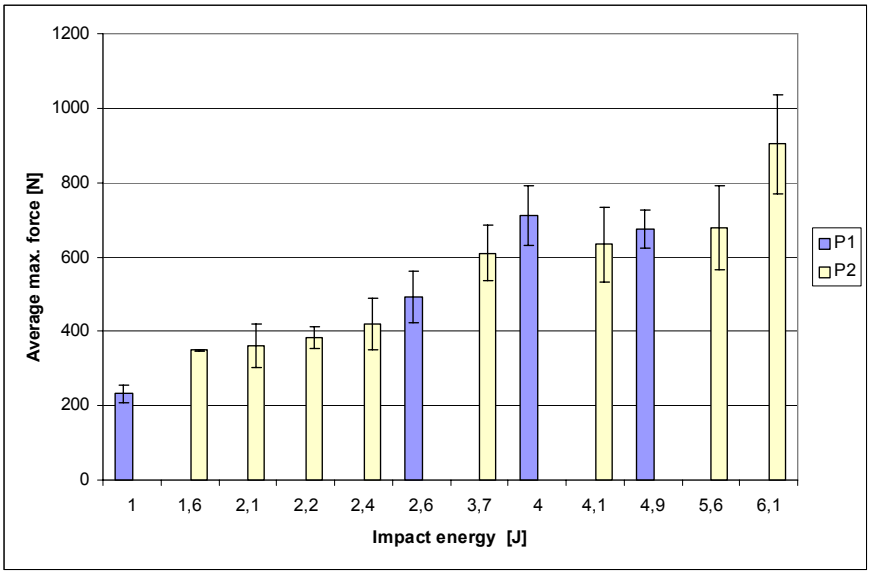

Figure 4: Average maximum forces including standard deviation for increasing impact energy for both pendulum masses used.

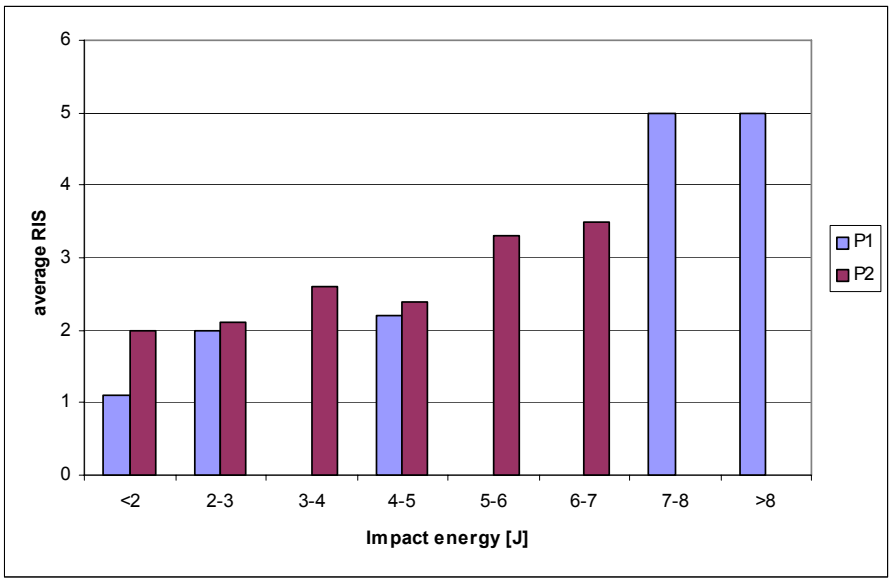

Figure 5: Average grade on the AAST renal injury scale for different impact energy intervals and different pendulum mass (see Appendix for detailed results).

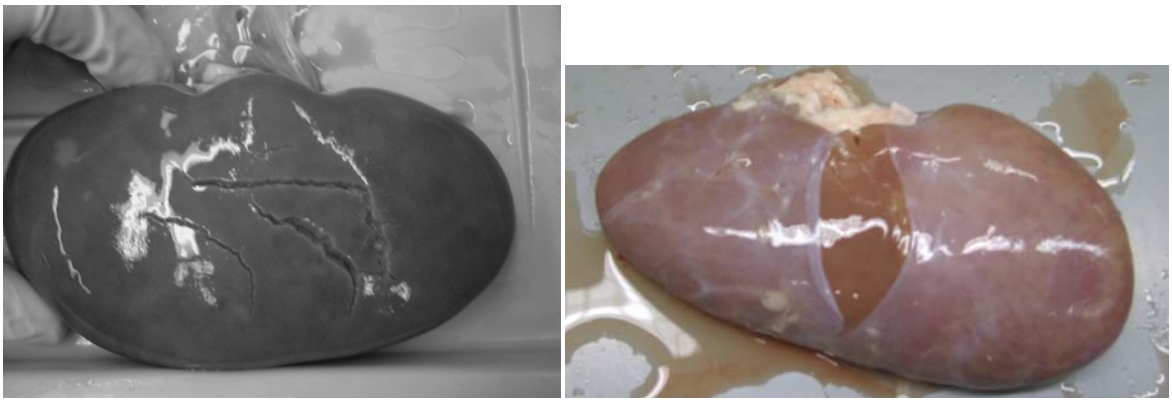

Figure 6: Typical injuries observed include rupture of the renal membrane (right) and the parchenyma (left).

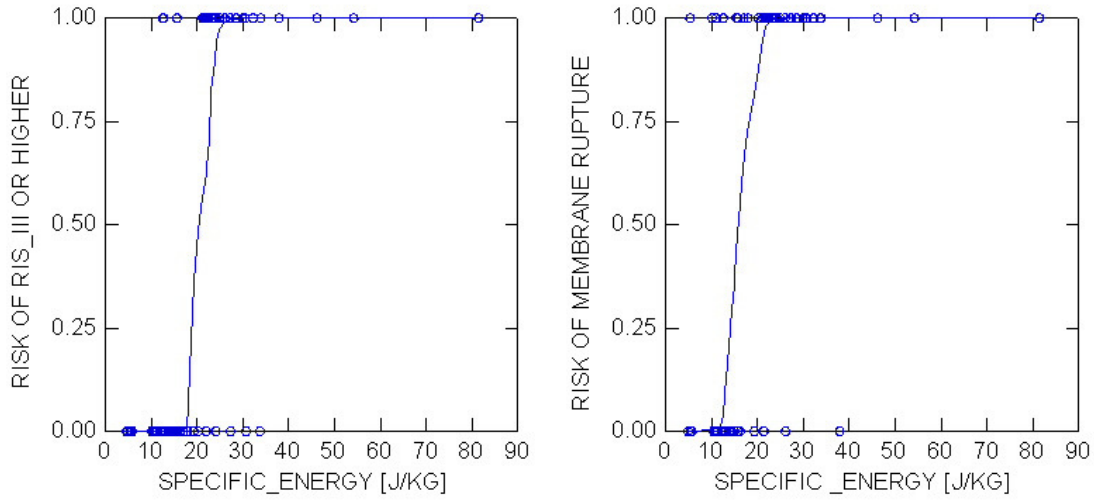

Figure 7: Risk curves illustrating the risk of AAST grade III or higher renal injury (left) and membrane rupture (right), respectively. Assuming a density of 1000 kg/m^3, the units of the specific energy can be transferred to energy density units [kJ/m^3].

Injury grade results were then used to develop different injury risk curves. The risk of sustaining an injury graded equal or higher than RIS III, as well as the risk of sustaining a rupture of the capsular membrane were determined with respect to the specific engery (i.e. the ratio of the impact energy divided by the mass of the kidney tested). The risk curves were determined using a Lowess fit (Figure 7). It emerged that a specific energy of 21 J/kg corresponds to the 50% risk of sustaing a RIS III or higher injury. Similarly a specific energy of 16 J/kg corresponds to the 50% risk of sustaining a membrane rupture. Assuming a density of 1000 kg/m^3 for the renal soft tissue the specific energy can be transferred into energy density which is a more common unit. Thus the thresholds become 21 kJ/m^3 and 16 kJ/m^3, respectively, and can more easily be compared to other studies, particularly those reporting strain energy densities associated with failure.

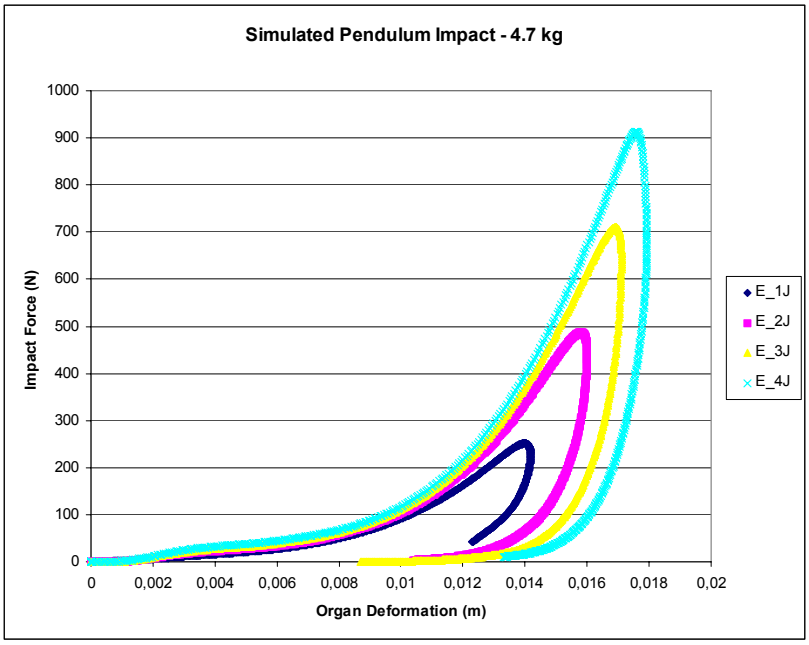

Figure 8: Force-deformation characteristics calculated by the FE model for different impact energies show similar behavior as the experiments.

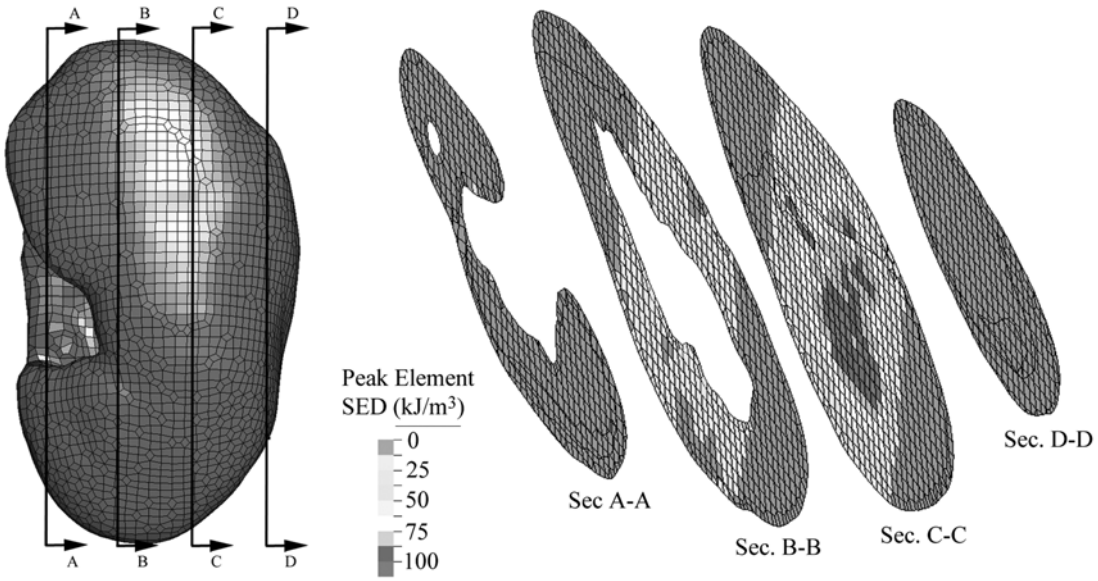

Figure 9: Time history of peak strain energy density level within various regions of the renal parenchyma during impact at 4J. The peak SED for each individual finite element over the course of the entire impact is superimposed on the non-deformed organ geometry.

In order to investigate the mechanisms underlying renal injury, a detailed and previously validated finite element model of human renal system was implemented. The simulated force-deformation response of the impacted kidney was found to correspond closely to those observed in the experiments. As expected, the predicted organ force-deformation behavior was sensitive to the impact energy level, with impact force increasing with increasing impact energy (Figure 8). The strain energy density (SED) magnitudes and distributions predicted by the simulations were generally consistent with the experimentally observed injury patterns. Strain energy density within the renal parenchyma was predicted to exceed known injury thresholds (40-60 kJ/m^3) for all simulated impacts above and including 2J, implying that the parenchyma would begin to lacerate at even this relatively low impact energy. Figure 9 illustrates the time history of peak SED within individual renal parenchyma finite elements in a 4J impact. It can be seen that a large region of the renal parenchyma is subjected to SED levels above 60 kJ/m^3. As impact severity progressively increased, more and more of the renal parenchyma was predicted to reach levels of strain energy density associated with failure, as can be seen in Figure 10, which shows the mean SED in the renal parenchyma as a function of impact energy. Furthermore, the FE simulations indicated that the renal capsule was predicted to first rupture at an applied impact energy of 4.0J, a level consistent with experimentally observed membrane ruptures (Figure 11). Both the dorsal and ventral surfaces of the renal membrane were predicted to reach a failure stress of 12 MPa (Figure 12).

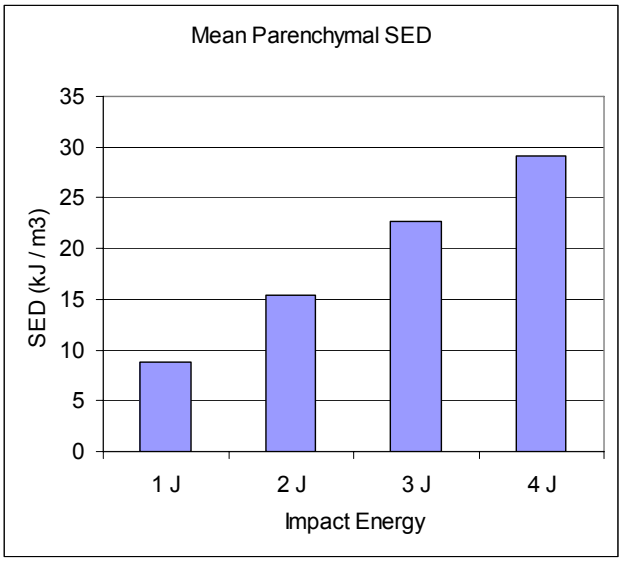

Figure 10: The mean SED within the renal parenchyma increases with increasing impact severity.

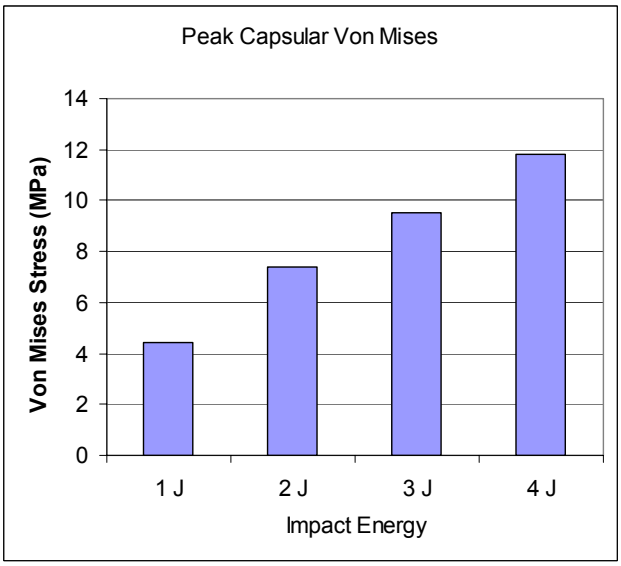

Figure 12: Peak stresses in the renal capsular membrane reach failure thresholds for impact energies above 4J.

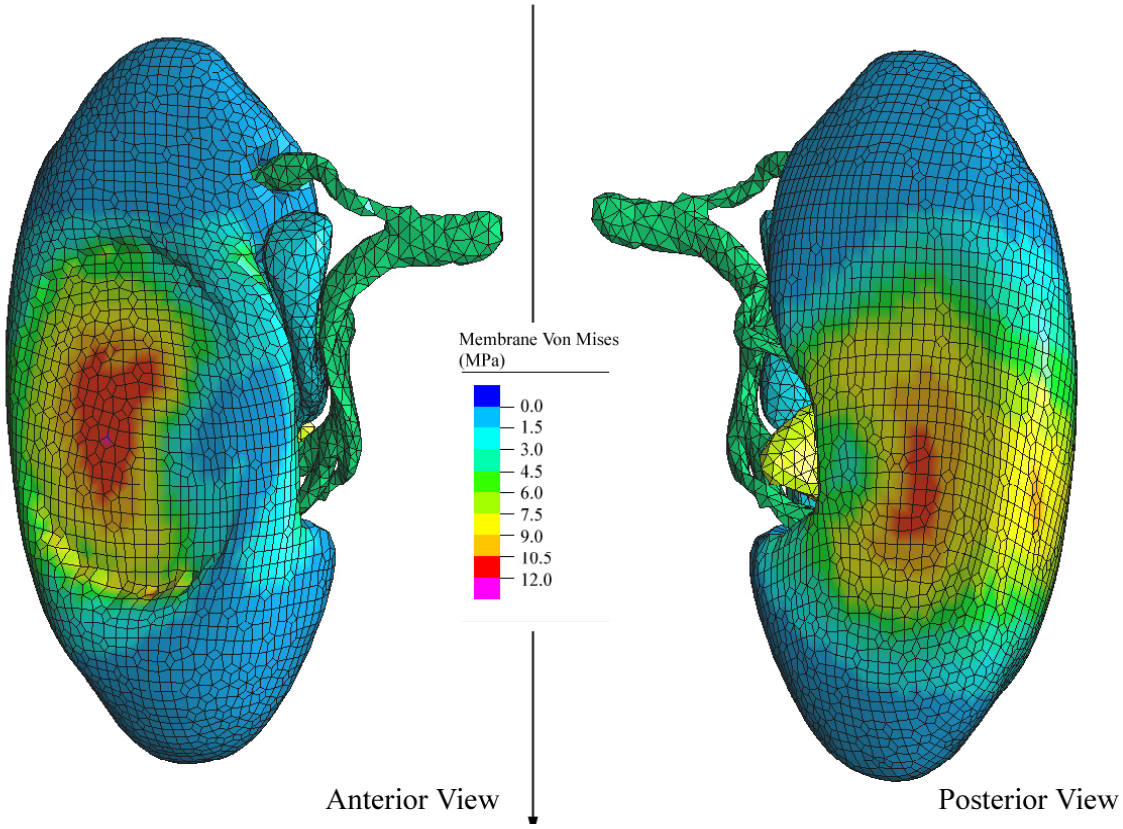

Figure 11: The renal capsular membrane was predicted to first reach failure stress thresholds at an impact energy of 4J. The membrane was predicted to rupture on the dorsal surface (directly beneath the impactor face), and also approached failure thresholds on the ventral surface. It is likely that failure of the renal membrane is a critical factor in the resulting injury severity.

DISCUSSION

In this study, the biomechanical response of kidneys to dynamic impact was investigated. The data elucidate certain mechanical aspects of renal trauma and are of particular importance for soft tissue modeling approaches. A pendulum impact device was used to load the kidneys and thus to determine the biomechanical response to traumatic loading. This methodology is reasonable, well established and commonly used in material testing. Using a specially designed set-up, it was possible to impact perfused, isolated kidneys with a loading that approximates external trauma to the *in vivo* kidney. The role of gravity in the current methodology corresponds to a standing or sitting person. Thus gravity acts perpendicularly to the impact axis, and the impactor is free to move without gravity as a causal force. In contrast, in other studies like Bschleipfer et al. (2002) which use drop tests (i.e. dropping a weight on the organ), the effects of gravity are always inherent in the results. This influence confounds analysis of mechanical behavior, specifically the determination of peak force and identification of unloading characteristics. This problem is avoided by using a horizontal pendulum impact device in which gravity acts perpendicular to the loading axis of the impact.

After recording the biomechanical response, the force-deformation-characteristics were determined for each tested kidney. In all organ response curves a visco-elastic behavior was observed. This finding was expected, since nearly all soft biological tissue exhibits viscoelasticity [Fung 1993]. In general, the kidneys showed a slowly increasing resistance to initial organ deformation followed by a fast ramping of

resistance up to the maximum force. Progressing further along the loading curve, the force magnitude drops despite a continued increase in organ deformation. From this behavior organ injury may be inferred since a force less than the maximum is sufficient to further deform the organ. Upon reaching the maximum deformation, the motion of the pendulum reverses direction. The kidney is subsequently unloaded as the pendulum moves away from the organ. During this phase, the parenchymal tissues rebound due to stored elastic energy. Consequently a portion of the organ deformation is reversible. However, the degree to which the tissues rebound depends on the grade of injury and the amount of remaining uninjured tissue, respectively. The force-deformation curves determined at different energy levels clearly reflect this behavior. As already mentioned above, vertical drop test methods are unable to properly observe the organ unloading phase.

The injuries observed and recorded during macroscopic investigation were in accordance with other studies [e.g. Bschleipfer et al. 2002]. Lesions primarily emerged at the center of the organ, in the vicinity of the impact location. The extent of injury was well correlated with impact energy. Generally, higher impact energy accounted for a higher injury score. But with regard to the curves presented in Figure 2, it should be noted that this effect was not seen when comparing force-deformation characteristics between the 4.0 J and 4.9 J level. One possible explanation for this phenomenon is that when the organs are impacted above a critical energy threshold, the underlying tissues fail at a relatively consistent force level. This result may also be attributed to the fact the curves at higher energy levels exhibited a larger variability. Further, it was found that at 4.9 J the lesions were distributed over a larger area, possibly dissipating more impact energy, and thus reducing the maximum force. It should be noted, however, that a larger area of injury does not necessarily result in a higher grade on the injury scale used. In other words, a large number of small lacerations, while certainly influencing the biomechanical response, will not necessarily qualify for a higher injury grade in the scaling scheme used here. Finally, as with many such experimental studies on biological soft tissues, the inherent variability of the organs and the size of the test population present a limitation which makes the conclusive interpretation of smaller differences in the results impossible.

With regard to the definition of an organ injury threshold, Bschleipfer et al.(2002) report that below a value of 4.0 J only a small area of the central craniocaudal third of the kidney showed injury while at energy levels above 4.0 J the area of detectable lesions measured more than 60% of the length of the organ. Despite the implementation of a different methodology to impact the kidneys, the current study lends support to the establishment of a 4.0 J renal injury threshold, which was determined to correspond to a grade III injury according to the AAST injury scale (see Appendix for corresponding AIS grades). This outcome is also in line with clinical observations by Santucci et al. 2001 who found that surgical intervention was required for only 15% of grade II injuries, but for 76% of grade III injuries. This is a strong indication that the biomechanical threshold of 4.0 J is also clinically relevant.

It should be noted that the establishment of a 4.0J energy injury threshold, whether for diagnostic purposes or for the development of preventative countermeasures, means little without considering the loading case. A human cadaver impact study performed by Walfisch et al. (1980) showed that a fall from a height of between 1 m and 2 m onto a rigid protrusion would transfer sufficient energy to the kidney to initiate renal damage, however the extent of organ injury was not reported. Another impact study by Viano (1989), showed that blunt impact with a large (23.5 kg, 15 cm diameter) impactor centered at the level of the ninth rib first caused renal injuries in laterally struck human cadavers at impact velocities between 5 and 7 m/s, or a total energy input to the body of between 300 and 575 J. This illustrates the extent to which the various structures of the body absorb and dissipate energy, and how the relatively defensive retroperitoneal positioning of the renal body in the abdomen protects it from trauma. It also illustrates the difficulty in predicting how an external impact, even with known energy and impactor geometry, will translate to renal injury. This is where numerical abdominal trauma models become important.

It is clear that the load case considered in the present study is abstract, and not directly indicative of traumatic injury that will occur in the field. First, the kidney is isolated from its surrounding tissues, which lend support to the kidney body, and effectively share in distributing applied loads. Secondly, the

kidney is most likely to be impacted by a fractured rib (Snedeker et al. 2005c) rather than a larger, blunt faced impact surface. However, the advantage to the applied load case, as can be seen in Figure 2, is that the impacts are repeatable. Such experiments with carefully controlled boundary conditions provide a critical experimental benchmark for the validation of numerical trauma models, such as the one used in this study. When well defined mechanical tests are used in combination with well designed numerical models, they can provide otherwise unobtainable insight into injury mechanisms, and yield information about appropriate injury thresholds. After organ level failure behavior has been quantified, the effects of the surrounding structures (such as the ribcage) can later be considered through the use of abdominal models.

Several numerical abdominal trauma models of varying detail and accuracy have been developed and reported in the literature [Iwamoto et al. 2002, Lizee et al. 2002, Lee and Yang 2001, Plank et al. 1998]. A more recent and relatively sophisticated model for the prediction of renal injury has been developed within our laboratory [Snedeker et al. 2002, 2005c], and validated against the previously mentioned human cadaver impact studies. By employing a 4.0 J renal injury criteria, this model predicts the first clinically significant renal injury to occur at an impact velocity of 6.1 m/s in the loading case of Viano. This result is in close agreement with the actual human cadaver impact experiments and illustrates that validated models may eventually provide a powerful tool for accurately predicting renal injury over a wide range of traumatic insults to the abdomen.

The finite element simulations employed in the present study provide useful insight into the mechanisms that underlie renal injury. First, and perhaps most important, the model predicts the renal capsule to rupture at impacts of 4.0 J and higher. The simulations showed that both the dorsal and ventral surfaces of the renal membrane would reach a failure stress of 12 MPa, a level established in previous studies of renal capsule failure behavior [Snedeker et al. 2005]. It is probable that a catastrophic failure of the membrane would result in severe, concomitant laceration of the underlying renal parenchyma. It is thus likely that failure of the renal membrane is the critical factor in the resulting injury severity. Such a failure would result in an AAST injury level III or above, and capsule rupture is often a primary clinical indication for surgical intervention [Smith et al. 1993, Schmidlin et al. 1998].

The FE model also provides important clues as to the manner in which the parenchymal tissues fail. However, it should be noted, that since tissue damage was not considered within the applied material models, only the initiation parenchymal laceration can be reliably predicted. The chain of events following the initial organ failure cannot be forecast with certainty. However, it was clear that the predicted concentrations of SED in the parenchymal finite elements did correspond to experimentally observed lesion patterns. Further, the observed SED distributions for impacts above 4.0 J are consistent with the higher number and severity of parenchymal lesions observed in this study, and previous studies [Bschleipfer et al. 2002].

Analyzing and discussing the results of this study, some limitations must be considered. First it should be noted that kidneys isolated from the body, at room temperature will behave differently than kidneys in an *in vivo* condition. Although the kidneys were perfused during testing to ensure a close to physiologic internal pressure of the organ, the interaction with the surrounding abdominal tissue was not considered in this work. Secondly, while a relatively large number of organs were tested, and we are confident that the indicated trends are representative of the biomechanical response of the kidney to traumatic impact, the experimental and biological variability inherent in these tests necessitate a larger sample size to attain statistically unambiguous results. Finally, the tests were performed on porcine kidneys, and caution must be applied when interpreting these results with regard to human safety.

Currently additional pendulum impact experiments are being performed using human kidneys. Preliminary results show a similar behavior of the human kidney indicating that the porcine model used here is reasonable. However, the number of human kidney tests conducted so far is not yet large enough to allow a sound statistical anlaysis.

CONCLUSIONS

The biomechanical response of porcine kidneys was investigated by performing pendulum impact experiments on isolated, perfused kidneys. The force-deformation curves were derived for various energy levels and different impact velocities. A finite element model was used to identify organ injury mechanisms, and the rupture of the renal capsule was identified as a potentially critical factor in the onset of severe renal injury. After impact, the observed lesions were rated using the AAST kidney injury scale. Hence a correlation of the biomechanical data to renal injury was established. For this study the following main conclusions can be drawn:

- The kidney tissue exhibits visco-elastic behavior.
- The mechanism of blunt impact seems to be predominately energy driven.
- An energy level of about 4.0 J can be regarded as a threshold value for renal membrane rupture
- An energy level of about 4.0 J can also be regarded as a threshold value for an AAST grade III renal injury which corresponds to AIS 3 injury.
- A strain energy density of 16kJ/m^3 corresponds to the 50% risk of sustaining membrane rupture; a strain energy density of 21kJ/m^3 corresponds to the 50% risk of sustaining an AAST grade III or higher kidney injury.

REFERENCES

AAAM. AIS: the injury scale (Eds. Gennarelli T and Wodzin E). Association of Advancement of Automotive Medicine (AAAM), USA, 1990/1998Update

Bozeman C, Carver B, Zabari G, Caldito G, Venable D. Selective operative management of major blunt renal trauma. J Trauma 2004; 57, 305-309.

Bschleipfer T, Kallieris D, Hauck EW, Weidner W, Pust RA. Blunt renal trauma: biomechanics and origination of renal lesions. Eur Urol 2002; 42: 614–621.

Farshad M, Barbezat M, Flüeler P, Schmidlin F, Graber P, Niederer P. Material characterization of the pig kidney in relation with the biomechanical analysis of renal trauma. J Biomech 1999; 32(4): 417-425.

Fung YC, Biomechanics: Mechanical Properties of Living Tissues, ed. 2, New York, Springer, 1993.

Iwamoto M, Kisanuki Y, Watanabe I, Furusu K, Miki K, Hasegawa J. Development of a finite element model of the Total Human Model for Safety (THUMS) and application to injury reconstruction. Proc. IRCOBI Conf, 2002.

Lee JB, Yang KH. Development of a finite element model of the human abdomen, The Stapp Car Crash Journal 2001; 45:79-100.

Lizee E, Robin S, Song E, Bertholon N, Le Coz JY, Besnault B, Lavaste F. Development of a 3D Finite Element Model of the Human Body, SAE Paper No. 983152, USA.

Melvin JW, Stalnaker RL, Roberts VL, Trollope ML. Impact injury mechanisms in abdominal organs. Proc. 17th Stapp Car Crash Conference 1973, SAE Paper No. 730968.

Mendis KK, Stalnaker RL, Advani SH. A constitutive relationship for large deformation finite element modelling of brain tissue. J Biomech Eng 1995; 117: 279-85.

Miller K. Constitutive modelling of abdominal organs. J Biomech 2000; 33(3): 367-373.

Moore EE, Cogbill TH, Malangoni MA, Jurkovich GJ, Shackford SR, Champion HR, McAninch JW. Organ injury scaling. Surg Clin North Am 1995; 75(2):293-303.

Nahum A, Melvin J. Accidental injury – biomechanics and prevention, ed.2, New York, Springer, 2002.

Plank GR, Kleinberger M, Eppinger RH. Analytical Investigation of Driver Thoracic Response to Out of Position Airbag Deployment, Proc. 42nd Stapp Car Crash Conference, USA, 1998.

Santucci R, McAninch J, Safir M, Mario L, Service S, Segal M. Validation of the American Association for the Surgery of Trauma organ injury severity scale for the kidney. J Trauma 2001; 50 (2): 195-200.

Santucci R, McAninch J. Grade IV renal injuries: evaluation, treatment and outcome. World J Surg 2001; 25: 1565-1572.

Schmidlin F, Schmid P, Kurtyka T, Iselin CE, Graber P. Force transmission and stress distribution in a computer-simulated model of the kidney. J Trauma 1996; 40: 791-796.

Schmidlin FR, Iselin CE, Naimi A, Rohner S, Borst F, Farshad M, Niederer P, and Graber P. The higher injury risk of abnormal kidneys in blunt renal trauma. Scand J Urol Nephrol 1998; 32: 388-392.

Schmitt K-U, Niederer P, Walz F. Trauma biomechanics – introduction to accidental injury, Heidelberg, Springer, 2004.

Smith, E. M., Elder, J. S. & Spirnak, J. P. Major blunt renal trauma in the pediatric population: is a nonoperative approach indicated? J Urol 1993; 149: 546-548.

Snedeker JG, Bajka M, Hug JM, Szekely G, Niederer P. The creation of a high-fidelity finite element model of the kidney for use in trauma research. J Visualization and Computer Animation 2002; 13:53-64.

Snedeker JG, Niederer P, Schmidlin FR, Farshad M, Demetropoulos CK, Lee JB, and Yang KH. Strain-rate dependent material properties of the porcine and human kidney capsule. J Biomechanics 2005a; 38: 1011-1021.

Snedeker JG, Barbezat M, Niederer P, Schmidlin FR, and Farshad M. Strain energy density as a rupture criterion for the kidney: impact tests on porcine organs, finite element simulation, and a baseline comparison between human and porcine tissues. J Biomechanics 2005b; 38: 993-1001.

Snedeker JG, Farshad M, Niederer P, Farshad M,. Biomechanics of renal trauma: Understanding injury through numerical simulation. In: Recent Research Developments in Biomechanics, 2 , S.G. Pandalai ed. Transworld Research Network Publishing, Kerala India 2005c.

Tamura, A.; Omori, K.; Miki, K.; Lee, J.B.; Yang, K.H. and King, A.I. "Mechanical Characterization of Porcine Abdominal Organs", Stapp Car Crash Journal 2002, 46: 55-69.

Viano DC, Lau IV, Asbury C, King AI, Begeman P. Biomechanics of the human chest, abdomen, and pelvis in lateral impact. Association for the Advancement of Automotive Medicine (AAAM), USA, 1989.

Walfisch G, Fayon A, Tarriere C, Rosey JP, Guillon F, Got C, Patel A, Stalnaker R. Designing of a dummy's abdomen for detecting injuries in side impact collisions. Proc. IRCOBI Conf., 1980.

Wessels H, Suh D, Porter J, Rivara F, MacKenzie E, Jurkovich G, Nathens A. Renal injury and operative management in the United States: results of a population-based study. J Trauma 2003; 54 (3): 423-430.

Yamada H. Strength of Biological Materials, Baltimore, Williams & Wilkins,1970.

APPENDIX -Table A: Test matrix and results.

Kidney No.	Pendulum 1: mass= 4,7 kg 2: mass=2,2 kg	Impact velocity [m/s]	Impact energy [J]	Injury grade RIS	Membrane rupture	Kidney weight [kg]
K1	1	0,64	1,0	I	n.a.	0,165
K2	1	0,64	1,0	I	n.a.	0,167
K3	1	0,64	1,0	I	n.a.	0,208
K4	1	0,64	1,0	I	yes	0,182
K5	1	2,30	12,5	V	yes	0,153
K6	1	1,87	8,2	V	yes	0,152
K7	1	1,44	4,9	II	yes	0,159
K8	1	1,06	2,6	II	yes	0,167
K9	1	0,64	1,0	II	no	0,168
K10	1	1,44	4,9	IV	no	0,187
K11	1	1,06	2,6	II	no	0,176
K12	1	0,64	1,0	I	no	0,196
K13	1	0,64	1,0	I	no	0,179
K14	1	1,06	2,6	II	no	0,186
K15	1	1,44	4,9	III	yes	0,188
K16	1	1,44	4,9	III	no	0,129
K17	1	1,06	2,6	II	yes	0,131
K18	1	1,44	4,9	II	yes	0,145
K19	1	1,06	2,6	II	yes	0,156
K20	1	1,44	4,9	III	yes	0,160
K21	1	1,06	2,6	II	no	0,163
K22	1	1,44	4,9	II	yes	0,179
K23	1	1,06	2,6	II	yes	0,172
K24	1	1,30	4,0	III	yes	0,133
K25	1	1,30	4,0	III	yes	0,139
K26	1	1,30	4,0	III	yes	0,167
K27	1	1,30	4,0	III	yes	0,171
K28	1	1,30	4,0	III	yes	0,176
K29	1	1,30	4,0	III	yes	0,180
K30	1	1,30	4,0	III	yes	0,188
K31	2	1,44	2,2	II	no	0,147
K32	2	1,44	2,2	III	no	0,176
K33	2	1,44	2,2	II	no	0,210
K34	2	1,88	3,7	III	no	0,175
K35	2	1,88	3,7	III	yes	0,116
K36	2	1,88	3,7	II	yes	0,155
K37	2	2,30	5,6	III	yes	0,121
K38	2	2,30	5,6	III	yes	0,165
K39	2	2,30	5,6	IV	yes	0,206
K40	2	1,20	1,6	II	yes	0,158
K41	2	1,37	2,1	II	no	0,158
K42	2	1,37	2,1	II	no	0,163
K43	2	1,37	2,1	II	no	0,185
K44	2	1,37	2,1	II	no	0,160
K45	2	1,37	2,1	II	yes	0,165
K46	2	1,37	2,1	II	yes	0,188
K47	2	1,37	2,1	II	no	0,195
K48	2	1,37	2,1	II	no	0,186
K49	2	1,48	2,4	II	no	0,173
K50	2	1,48	2,4	III	no	0,192
K51	2	1,48	2,4	II	no	0,196
K52	2	1,48	2,4	II	no	0,190
K53	2	1,48	2,4	III	yes	0,156
K54	2	1,48	2,4	II	yes	0,156
K55	2	1,48	2,4	II	no	0,200
K56	2	1,92	4,1	IV	yes	0,176
K57	2	1,92	4,1	IV	yes	0,182
K58	2	1,92	4,1	III	yes	0,169
K59	2	1,92	4,1	II	no	0,259
K60	2	1,92	4,1	III	yes	0,187
K61	2	1,92	4,1	II	no	0,211
K62	2	1,92	4,1	II	yes	0,228
K63	2	2,34	6,1	III	yes	0,214
K64	2	2,34	6,1	IV	yes	0,244
K65	1	1,24	4,1	II	yes	0,185